CENTER FOR PHYSICAL SCIENCES AND TECHNOLOGY

SEMICONDUCTORS PHYSICS INSTITUTE

VILNIUS UNIVERSITY

Gediminas Molis

INVESTIGATION OF THE TERAHERTZ PULSE GENERATION FROM THE NARROW BAND GAP SEMICONDUCTOR SURFACES

Summary of the doctoral thesis

Physical Sciences, Physics (02 P), Semiconductor Physics (P 265)

Vilnius, 2010

The research work was performed in 2005-2009 at the Optoelectronic laboratory of the Semiconductors Physics Institute

Scientific supervisor:

Prof. habil. dr. Arūnas Krotkus (Center for Physical Sciences and Technology Semiconductors physics institute, Physical sciences, Physics – 02 P, Semiconductor Physics – P265)

Council of defense of the doctoral thesis:

Members:

Habil. dr. Gintaras Valušis-chairman (Center for Physical Sciences and Technology Semiconductors physics institute, Physical sciences, Physics – 02P, Semiconductors Physics P265)

Prof. habil. dr. Valerijus Smilgevičius (Vilnius university, Physical sciences, Physics – 02P, Optics P200)

Prof. habil. dr. Gintaras Babonas (Center for Physical Sciences and Technology Semiconductors Physics Institute, Physical sciences, Physics – 02P, Semiconductors Physics P265)

Prof. dr. Artūras Jukna (Vilnius Gediminas Technical University, Physical sciences, Physics – 02P, Semiconductors Physics P265)

Dr. Viktoras Vaičikauskas (Center for Physical Sciences and Technology Physics Institute, Physical sciences, Physics – 02P, Semiconductors Physics P265)

Opponents:

Dr. Vytautas Karpus (Center for Physical Sciences and Technology, Physical sciences, Physics – 02P, Semiconductors Physics P265)

Prof. habil. dr. Sigitas Tamulevičius (Kaunas University of Technology, Physical sciences, Physics – 02P, Semiconductors Physics P265)

The official defense of the thesis will be held at conference hall in the Center for Physical Sciences and Technology, Goštauto 11, Vilnius on June 22 2010, 11 a.m.

Summary of the thesis was mailed on May … 2010. The doctoral thesis is available at Vilnius University and Center for Physical Sciences and Technology Semiconductors Physics Institute libraries.

FIZINIŲ IR TECHNOLOGIJOS MOKSLŲ CENTRO

PUSLAIDININKIŲ FIZIKOS INSTITUTAS

VILNIAUS UNIVERSITETAS

Gediminas Molis

TERAHERCINIŲ IMPULSŲ, GENERUOJAMŲ SIAURATARPIŲ PUSLAIDININKIŲ PAVIRŠIUJE, TYRIMAS

Daktaro disertacijos santrauka

Fiziniai mokslai, fizika (02 P), puslaidininkių fizika (P 265)

Vilnius, 2010

Darbas atliktas 2005-2009 m. Puslaidininkių fizikos institute Optoelektronikos laboratorijoje.

Mokslinis vadovas:

Prof. habil. dr. Arūnas Krotkus (Fizinių ir technologijos mokslų centro Puslaidininkių fizikos institutas, fiziniai mokslai, fizika -02P, puslaidininkių fizika – P265).

Disertacija ginama Vilniaus universiteto Fizikos mokslo krypties taryboje:

Nariai:

Habil. dr. Gintaras Valušis-pirmininkas (Fizinių ir technologijos mokslų centro Puslaidininkių fizikos institutas, fiziniai mokslai, fizika – 02P, Puslaidininkių fizika – P265)

Prof. habil. dr. Valerijus Smilgevičius (Vilniaus universitetas, fiziniai mokslai, fizika – 02P, Optika – P200)

Prof. habil. dr. Gintautas Babonas (Fizinių ir technologijos mokslų centro Puslaidininkių fizikos institutas, fiziniai mokslai, fizika – 02P, Puslaidininkių fizika – P265)

Prof. dr. Artūras Jukna (Vilniaus Gedimino Technikos Universitetas, fiziniai mokslai, fizika – 02P, Puslaidininkių fizika – P265)

Dr. Viktoras Vaičikauskas (Fizinių ir technologijos mokslų centro Fizikos institutas, fiziniai mokslai, fizika – 02P, Puslaidininkių fizika – P265)

Oponentai:

Dr. Vytautas Karpus (Fizinių ir technologijos mokslų centro Puslaidininkių fizikos institutas, fiziniai mokslai, fizika – 02P, Puslaidininkių fizika – P265)

Prof. habil. dr. Sigitas Tamulevičius (Kauno Technologijos Universitetas, fiziniai mokslai, fizika – 02P, Puslaidininkių fizika – P265)

Disertacija bus ginama viešame Fizikos mokslo krypties tarybos posėdyje Fizinių ir technologijos mokslų centro posėdžių salėje, 2010 m. birželio 22 d. 11val., adresu Goštauto 11, Vilnius.

Disertacijos santrauka išsiuntinėta 2010 m. gegužės ……d.

Disertaciją galima peržiūrėti Vilniaus universiteto ir Fizinių ir technologijos mokslų centro Puslaidininkių fizikos instituto bibliotekose.

Introduction and aims of the study

Terahertz radiation (THz) is a generic term for waves with a spectrum between 0.1 and 10 THz. Sometimes, the THz spectrum is defined as T-ray: especially in connection with imaging techniques. The frequency of 1 THz corresponds to a wavelength of 300 μm or 0.3 mm and to a wavenumber of 33 cm^{-1}: THz fields have wavelengths extending from 3 mm (0,1 THz or 100 GHz) up to 30 μm (10 THz). This wavelength interval ranges between the top edge of the millimeter wave spectrum and the bottom edge of the optical spectrum, and corresponds to the boundary of the far-infrared (FIR) spectral region.

When compared to microwave or optical ranges, THz technology isn't so well developed. Recently, remarkable progress is achieved using optoelectronic generation and detection methods of the broadband THz radiation. Also electrooptic method can be used for generation and coherent detection of the broadband THz radiation.

CW THz fields can be generated using Gunn diodes, photomixers, and various lasers. Gunn diode is a mono-polar semiconductor structure without *p*-*n* junctions. When biased to the voltages larger than the threshold, such diodes can generate CW electromagnetic radiation with frequencies up to 1THz. Gas lasers generate CW THz signals in the frequency domain 0.9–3 THz with output powers in the range of 1–30 mW. A gas laser consists of a carbon dioxide laser pump and a cavity filled with a gas such as CH4; N2; etc., which dictates the lasing frequency. The gas sources show no tunability and are very large. To detect CW THz radiation various bolometers, Golay cells, pyroelectric detectors and Schottky diodes can be used.

Every generation and detection method mentioned above has its applications. THz lasers and other CW radiation sources are most suitable for the imaging. Short THz pulses most often are used for Fourier absorption and reflection spectroscopy. The absorption spectra of many polar molecules, for example H_2O; C, N_2;O_2; O_3; HCl, CO, SO_2; CH_3CN; etc., have many, distinct spectral peaks in the THz range. These unique signatures of the molecules in the THz range is of highest importance in monitoring the surrounding medium, air pollution detection, gas sensing, drugs and explosives detection. THz scanning systems are already in operation in some airports for security purposes. One of most attractive THz applications is the detection of mural paintings covered with plaster. By measuring reflected THz light from the paint layers under the plaster, it is possible to get the hidden mural painting images in black and white. Also it is possible to get even the image of the sketch laying under the multiple paint layers.

Generation of THz pulses from semiconductor surfaces excited using femtosecond laser pulse has big potential for semiconductors properties investigation. THz radiation can arise because of many different mechanisms: screening of semiconductor surface electric field, photo-Dember effect, optical rectification (OR) and electrical field induced optical rectification effect (EFIOR), plasma waves and coherent phonons and plasmons. Investigating THz radiation generation mechanisms one can find out important semiconductor parameters such as index of refraction, mobility, charge carriers relaxation times, intervalley separation energy.

This work is focused on investigation of semiconductors properties generating THz pulses from various semiconductors surfaces. THz radiation generation mechanisms were investigated changing sample temperature, magnetic field, exciting laser wavelength and pulse duration.

Main goals

- Development of a THz Time domain spectroscopy system and the optimization of its optical and optoelectronic components.
- The search for the best THz surface emitter by the comparison various semiconductor materials and different THz surface emission mechanisms.

The objectives of the study

- Using photoconductive emitters and detectors made in Semiconductors Physics Institute, make THz generation and detection system from scratch. Adapt it for THz radiation surface emitters investigation experiments.
- Using the THz TDS system, investigate various surface emitters and compare them.
- Explore THz pulse amplitude dependences on intrinsic carriers' concentration and azimuthal angle for several different THz surface emitter materials.
- Investigate the dependences of the THz signal amplitude generated from various semiconductors surfaces on the excitation laser wavelength.

The novelty of the study

- THz pulses generations from various semiconductors surfaces have been thoroughly investigated.
- By using the THz excitation spectroscopy technique, the intervalley separation energies in the conduction band of $In_xGa_{1-x}As$ (x=0; 0.2; 0.53; 1) and InSb samples ware measured for the first time.

The defended propositions of the dissertational research

- Best surface emitter when using 800nm wavelength Ti:Sapphire femtosecond laser pulses for excitation is p-InAs ($p \leq 10^{17}$ cm^{-3}).

- THz radiation in the InAs surface mainly is generated because the photo-excited charge carriers move into the bulk with different speeds and electrical field is formed and latter part of the optical pulse is rectified due to an optical non-linearity that is induced by this field.
- THz radiation amplitude, generated in the semiconductor surface, depends on the excitation pulse wavelength; it has maximum from which position it is possible to calculate the intervalley energy separation in the conduction band of the material.

Outline of the thesis

The thesis consists of five chapters. **Chapter 1** is Introduction to the general character of THz radiation and its applications. There are briefly overviewed recent achievements in THz technology and future prospective.

Chapter 2 is dedicated to the detailed overview of pulsed THz radiation generation methods. Different THz pulse generation and detection methods (photoconductive switch, electrooptic crystal, etc.) are presented. Also various physical mechanisms of THz pulse radiation from the semiconductors surfaces illuminated with femtosecond laser pulses are analyzed in this Chapter.

The selection of a photoconductive emitter material is, generally, determined by the laser wavelength. The laser radiation must be absorbed as efficiently as possible in the photo-conducting part of the emitter. For example, when the Ti: sapphire laser emitting around 800 nm wavelength is used for the photoexcitation, best materials for the THz emitters are GaAs or Silicon on Saphire (SOS) layers. When exciting with ~ 1 μm and longer wavelengths femtosecond lasers, GaInAs, GaInSb or GaBiAs are used. For efficient THz radiation out-coupling through the semiconductor/air interface to the free space and

efficient THz pulse detection planar metallic antennae are used. The antennae are usually formed using photolithographic techniques. The antenna geometry is very decisive parameter for determining the radiant and registered frequency bands.

Most simple way to generate THz radiation is to illuminate an unbiased semiconductor surface with a femtosecond laser pulse. In such a case, THz radiation is generated because of several different physical mechanisms: the photo-current surge, the photo-Dember effect, the optical rectification (OR) or electrical field induced optical rectification (EFIOR) effects, and due to coherent generation of infrared active phonons and plasmons. Historically, the first explanation of the surface THz radiation effect in semiconductors illuminated with femtosecond pulses was the built-in surface electric field screening by the photoecited carriers (the current surge model). According to this model it was concluded that the generated THz radiation intensity must depend on the semiconductor doping level, because it affects the strength of the built-in surface electric field. Therefore, measurements of the THz radiation intensity dependence on its doping level were done by several groups. According to these measurements, the most intense THz radiation was generated by n-type GaAs crystals with the electron concentration of 3.5×10^{15} cm^{-3}.

Chapter 3 describes how the THz generation/detection system used in the experiments performed in this work. For all experiments, the coherent detection method was used. Femtosecond laser beam was divided by using a polarizer and a $\lambda/2$ waveplate into two separate parts. One part of the beam was focused onto the surface of semiconductor (sample) to generate THz pulse and the other beam part was used to illuminate photoconductive or electrooptic (Fig. 1) THz detector. THz radiation generated at semiconductor surface was radiated into free space. THz beam is diverging in free space. To collect it efficiently to the detector, a Teflon lens or off-axis parabolic mirrors were used.

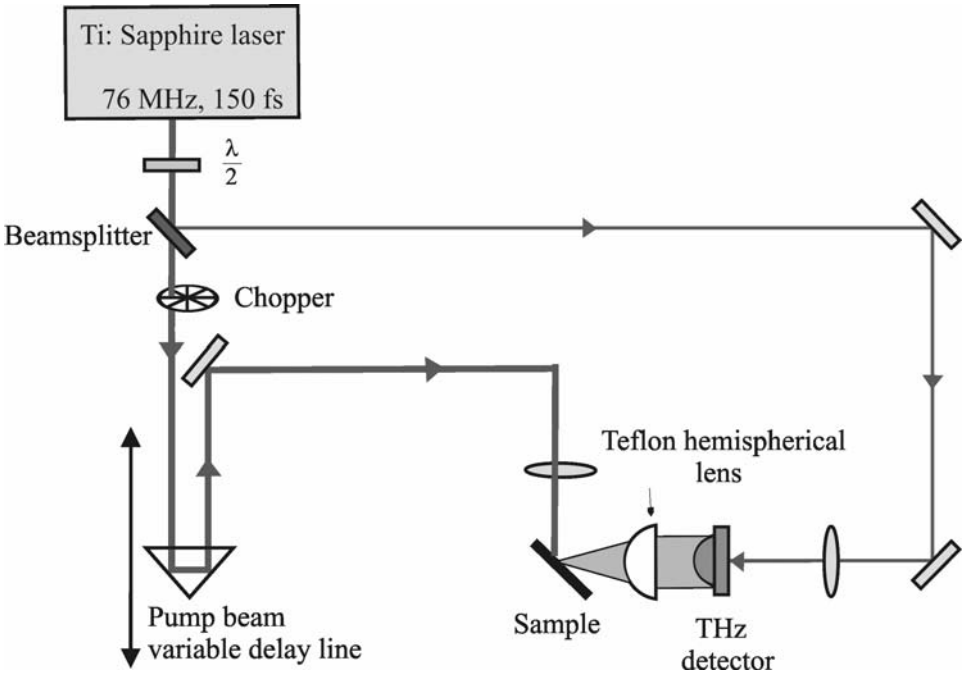

Fig. 1 Coherent detection scheme

When measuring radiation power dependence on azimuthal angle, sample was mounted onto 360^{o} rotary stage. The photoconductive detection method was the main registration technique and the electrooptic method was used only to measure THz radiation amplitude dependence on excitation laser wavelength.

THz radiation photoconductive detectors and emitters were made from low temperature (LT) grown GaAs. Layers of LT-GaAs were grown using molecular beam epitaxy (MBE) machine at the Semiconductors Physics Institute by Dr. K. Bertulis. Planar Ti/Au metal antennas were formed by using photolithographic processing processes under the guidance of Dr. S. Balakauskas.

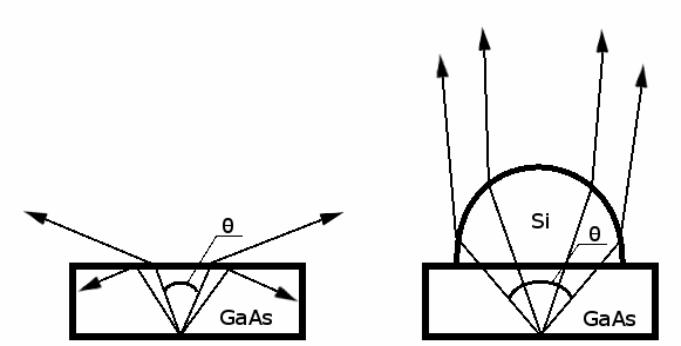

Fig. 2 Spherical lens effect on THz radiation emission to the free space.

GaAs used to fabricate photoconductive emitters and detectors has quite a large index of refraction (n~3.5). Therefore, a big part of THz radiation is reflected back at the semiconductor air interface to the bulk of semiconductor because of the internal reflection. In order to increase the THz radiation emission at the output of the device, hemi-spherical silicon lenses were used. Silicon was selected as the material for the lenses because it is transparent in the THz range and its refractive index is close to that of GaAs. Such spherical lens was attached to the backside of THz emitter or detector. It helps to increase the spatial angle of the out-coupled THz radiation (Fig. 2) and also focuses the beam. First silicon lenses (2-4 mm in diameter) were made by cutting silicon crystal to cube-shaped pieces and by placing them into the box with walls covered by an abrasive paper. When blowing the compressed air into the box, the cubic pieces were converted into the spheres. After that, one side of the Si-spheres was polished and hemisphere lenses were formed.

For subsequent experiments 15 mm diameter silicon lenses fitted into device mount together with the GaAs detector or emitter were used. A specially designed mount has a lens positioning option that was realized using two micro-positioning screws. When manufacturing silicon lenses of 15 mm in diameter, the thickness of the lens was chosen to collimate 1 THz frequency radiation. The purpose was to simplify the THz time domain (TDS) Fourier spectrometer optical scheme. When using collimating lenses no any additional optical elements are needed to focus THz radiation to the detector. When trying

to identify the most appropriate geometrical configuration of the photo-conductive emitter antennas, four different types of the antennas were tested (Fig. 3). Different geometric configurations were compared by measuring the Fourier spectra of the emitted THz pulses. After the tests, coplanar configuration antenna has been selected as the best solution for the emitters, because it has radiated most uniformly over a rather wide THz frequency range.

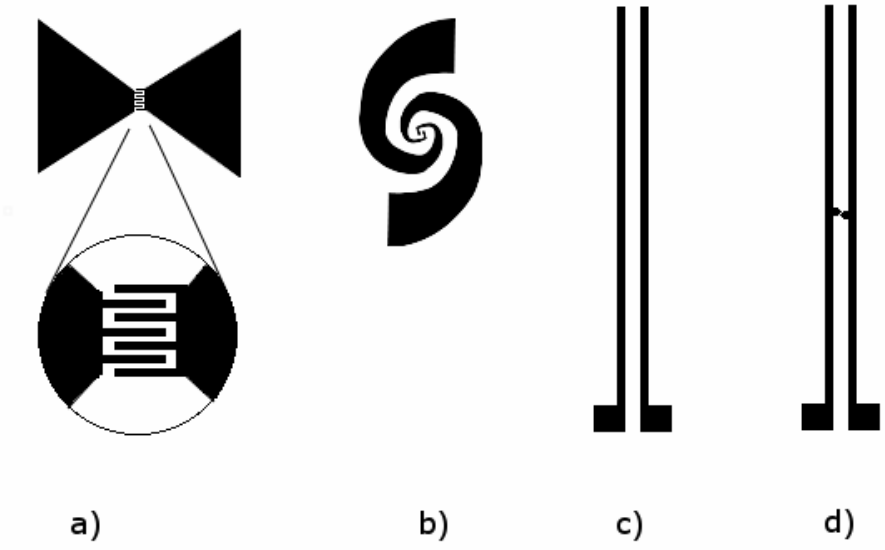

Fig. 3 Tested emitter antennas.

In order to increase the emitted THz radiation power, metal-semiconductor-metal (MSM) and p-i-p emitter structures were tested. The dependence on the bias voltage, and the photo-excitation intensity were investigated. The amplitude of the THz pulse emitted from a p-i-p structure saturates at rather low bias voltages (Fig. 4). This can be explained by the fact that this structure has the contacts that are blocking the electron flow from the cathode. Therefore, electrons from the metal are not injected into the active region and the current is transferred only by photoexcited electrons. The flow of the photoexcited electrons saturates, because the electron drift velocity saturates. On the other hand, in the MSM

structure, the amplitude of the radiated THz pulse is continuosly increasing with the increase of the bias and is limited only by the thermal breakdown of the structure. Therefore, in the subsequent investigations only MSM contact structures were used.

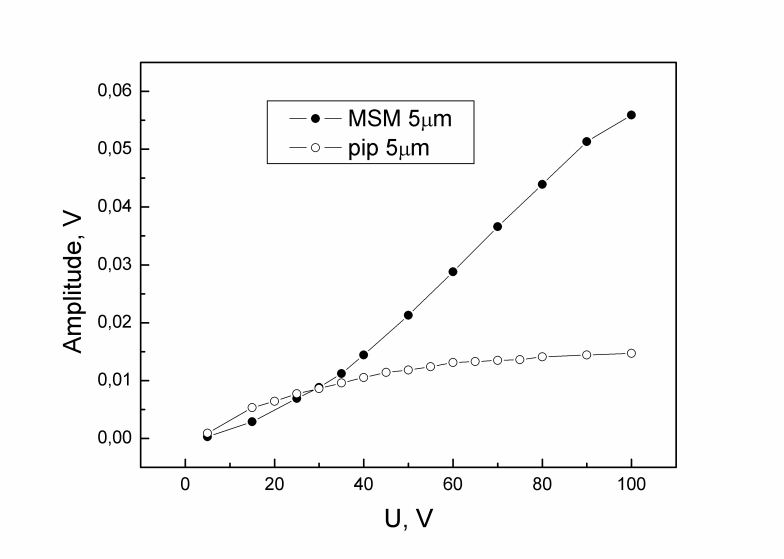

Fig. 4 THz radiation amplitude dependence on voltage applied to the MSM and pip structures.

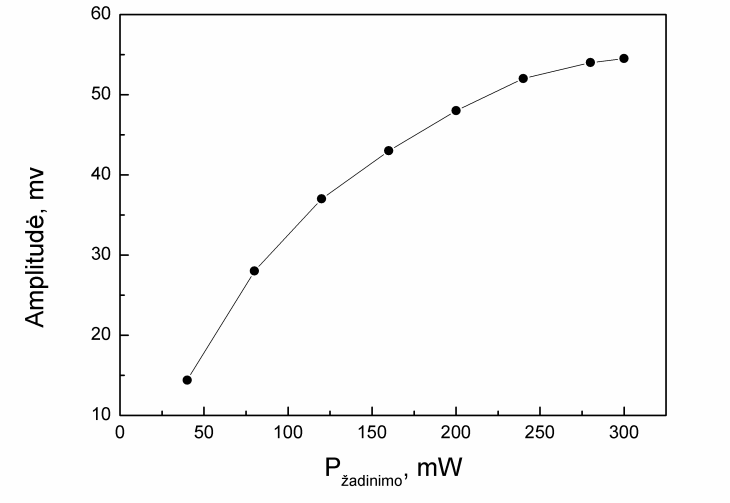

Fig. 5 Recorded THz electric field amplitude dependence on the laser radiation intensity at 100 volts applied to the contacts.

In subsequent experiments with the MSM structures, the emitted THz pulse amplitude dependences on the excitation intensity (Fig. 5) and on the bias voltage at different excitation levels (Fig. 6) were measured.

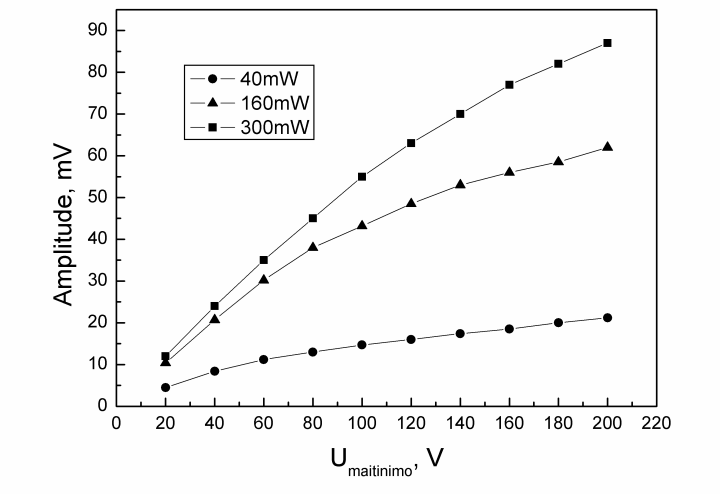

Fig. 6 Recorded THz electric field amplitude dependence on the bias applied to emitter contacts at different laser radiation intensity.

For MSM structure emitter, with 80 μm gap between contacts, the THz signal amplitude saturates when the average laser power reaches ~300 mW. This saturation may be caused by the electric field screening by the photoexcited carriers. The experiments show that, when working at high voltages and excitation intensities, the emitter lifetime is drastically reduced due to its thermal breakdown.

The most important parameter for the THz detector is the charge carriers lifetime in the epitaxial layer of LT-GaAs. This lifetime determines the maximum frequency that can be registered by the device. Reduction of the photoexcited carriers capture time increases spectral bandwidth of the THz-TDS system, but it also reduces the detector sensitivity. It is very important to determine what charge carriers lifetime is optimal to register the widest possible spectrum simultaneously having the best signal-to-noise ratio (the latter parameter depends on the sensitivity of the detector).

When experimentally determining the optimal capture time of the charge carriers, an epitaxial LT-GaAs layer grown on semi-insulating GaAs substrate was used. First of all planar detector antennas were formed, then the wafer was cut into separate chips that were annealed at the temperatures of 500°, 550°, 600°, and 700° C in the rapid thermal annealing oven for 30 s. Since the detector spectrum maximum frequency may be limited by the laser pulse duration (Fig. 7), for the spectral width measurements Ti: sapphire laser with 15 fs pulse duration was used.

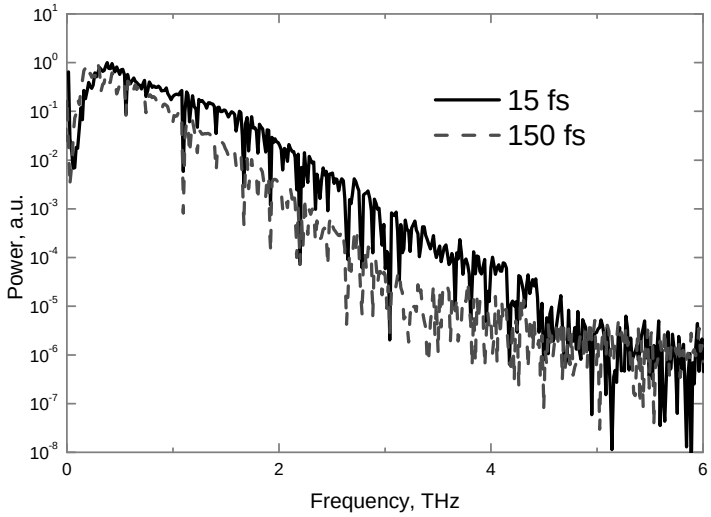

Fig. 7 Registered FFT spectrum by photoconductive detector using two different laser pulse durations.

The detector annealed at 700°C registers up to 10 times greater signal amplitude as compared with the detector annealed at 500°C (Fig. 8). A comparison of the Fourier spectra (Fig. 8) shows that, after the increase of the annealing temperature, the frequency bandwidth of the THz-TDS system decreases. The bandwidth of the system that has a detector annealed at

500°C reaches the spectral bandwidth of 4 THz, whereas for the detector annealed at 700°C this bandwidth is only of the order of 2 THz.

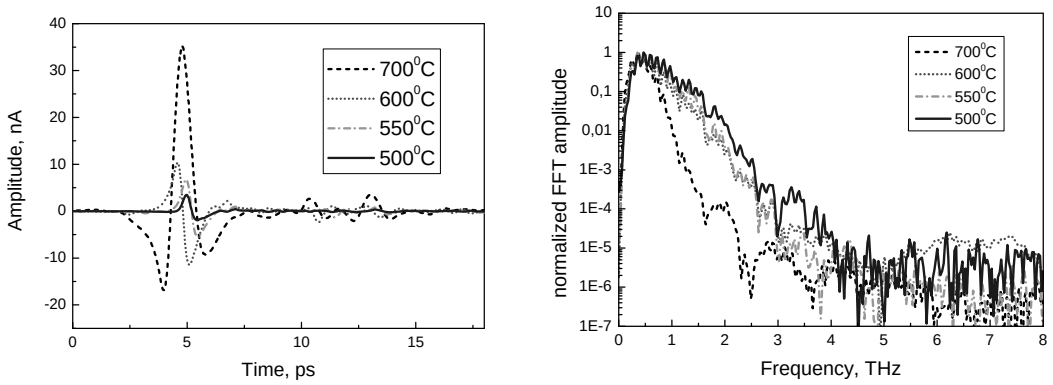

Fig. 8 Registered amplitude and FFT spectrum dependence on annealing temperature.

Depending on the purpose, for which the system will be used, the detector annealing temperature must be selected. THz spectroscopy measurements require a broad spectrum, so the detectors can be annealed at lower temperatures 500-550°C, in this case. For optical pump-THz probe experiments a more sensitive detector is desirable, and the spectrum broadness in this case is less relevant. For the latter experiment, detectors should be annealed at higher temperatures of ~ 700°C.

Currently, the most common solid-state femtosecond laser is a Ti: sapphire laser optically pumped by the second harmonics of the Nd: YAG laser radiation. Nd: YAG laser, in turn, is pumped by the laser diode array. The resulting four-stage laser system is both costly and complicated. After femtosecond solid-state and fiber lasers (emitting 1-1.5 μm wavelength) directly pumped by laser diodes were developed, there is a need to produce photoconductive THz radiation detector suitable for such lasers. GaAs in this case is not suitable because of its absorption edge is ~ 0.9 μm, so this material does not absorb the longer wavelength radiation. Photoconductive detectors sensitive to 1-1.5 μm radiation can

be produced from the ion-implanted InGaAs, low-temperature grown GaAsSb, and GaAsSb. The low temperature grown GaBiAs epitaxial layers have quite a large resistivity and short lifetime of charge carriers (up to 1 ps). As GaBiAs absorption edge is in the infrared spectrum, this material is ideal for the manufacture of the photoconductive detectors designed to operate in pair with 1-1.5 μm wavelength femtosecond laser.

After initial test of the detector made from GaBiAs with 800 nm wavelength Ti:Sapphire laser, the experiments with 1030 nm wavelength femtosecond laser "Pharos", produced by the “Light conversion” have started. "Pharos" is a solid-state laser with Yb: KGW (KGD (WO3)) crystal directly pumped by the laser diode array. The average radiation power of the laser is 600 mW, the pulse duration 63 fs, and the spectrum FWHM (full width at half maximum) 28 nm. THz radiation was generated by n and p-type crystals of InGaAs and InN surface emitters and GaBiAs photoconductive emitter. THz radiation from semiconductor surfaces of InN were generated in a reflection geometry, and in the InGaAs case, in a transmission geometry. In addition 1 cm diameter spherical Teflon lens was used to focus THz radiation to the detector. 70 mW of laser power was directed to the detector and the remainder of the power used to generate the THz radiation from semiconductor surfaces. Using Yb: KGW femtosecond laser registered spectrum reaches only 2 THz, while in the case of the Ti:Sapphire laser it was up to 3 THz. This could be explained by the higher frequency THz radiation absorption in GaAs hemispherical lens (as opposed to 800 nm laser systems GaAs lens was used to focus THz radiation to the detector on the assumption that in the silicon lens photo generated charge carriers due to the long relaxation time would lead to decrease of the permeability in THz range).

Chapter 4 describes the experiments done during the doctoral studies to find the best surface emitter and to find out what is the main mechanism of the THz pulses generation. THz radiation emission from a variety of narrow bandgap (n-InAs, p-InAs, InSb, GaSb, Te, HgTe, various compositions of $Cd_xHg_{1-x}Te$ and $In_xGa_{1-x}As$) and wide bandgap (GaAs, Ge)

semiconductors, and chalcogenides (CuInSe2 , CuInS2, CuInGaSe2) was investigated. The samples were illuminated by Ti:sapphire laser (pulse duration - 150 fs, repetition rate - 76 MHz, the central wavelength - 800 nm, the average radiated power - 500 mW). Generated THz pulses were recorded using photoconductive LT-GaAs detector as described in **chapter 3**. Some of the investigated semiconductors ($Cd_xHg_{1-x}Te$) were evidenced to generate THz pulses for the first time. As it is seen from Fig. 9 the best surface emitter found for Ti:Sapphire laser is p-doped InAs.

To find out what doping level is the best for InAs surface emitter, samples made from twelve InAs n-and p-type single crystals with the doping levels varying between 10^{16} and 10^{19} cm^{-3} were investigated. THz emission was observed from mechanically polished (111) surfaces. 150 fs duration, 76 MHz repetition rate, and 810 nm central wavelength pulses from a mode-locked Ti:sapphire laser were used for the sample excitation; THz radiation was collected by an ultrafast photodetector with dipole antenna and a substrate lens from high resistivity silicon crystal. The detector was oriented to prevailingly register TM polarization of the radiated emission.

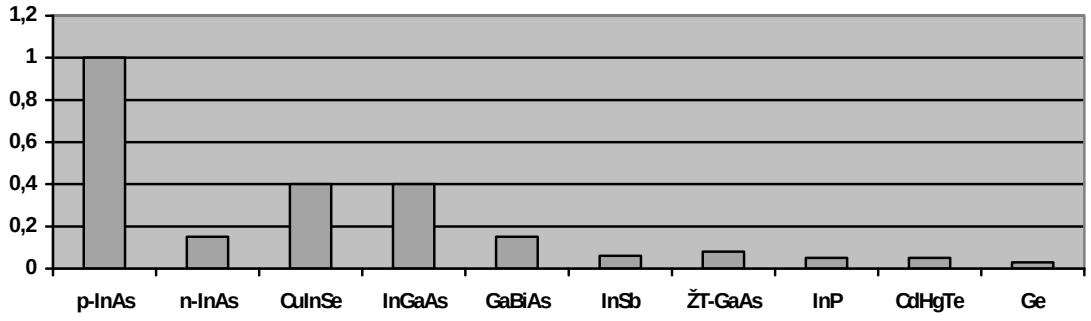

Fig. 9 Comparison of the amplitude of THz radiation generated by various surface emitters excited with 800 nm wavelength, 150 fs duration Ti: sapphire laser pulses.

Figure 10 shows the dependence of the emitted THz field magnitude on the crystal doping level. It can be seen from the figure that there is a strong enhancement of the radiated field magnitude corresponding to p-type doping levels of 10^{16}–10^{17} cm^{-3}.

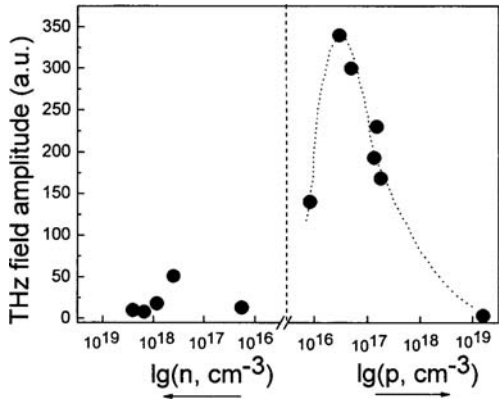

Fig. 10 Dependence of the emitted THz field magnitude on the InAs crystal doping level (dotted line is a guide for the eye).

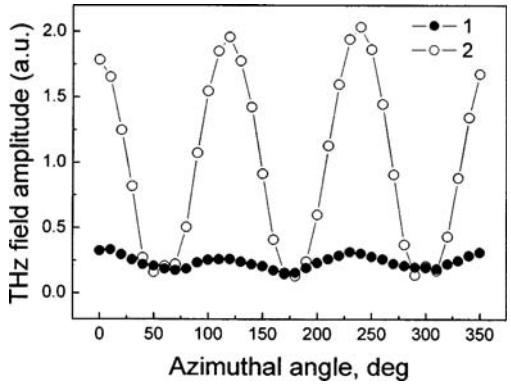

Fig. 11 Azimuthal angle dependencies of THz radiation emitted from the surfaces of two InAs samples with different doping levels: n=1.8x10^{16} cm^{-3} (1) and p=3x10^{16} cm^{-3} (2).

The shape of THz transients recorded in the range with the largest magnitudes is very sensitive to the azimuthal angle of the sample orientation around the axis normal to the surface. This is demonstrated by two azimuthal dependencies shown in Fig. 11. For the

sample with p-doping level from the range with the maximal THz amplitudes, azimuthal dependence is very pronounced the ratio of the signals at the angles corresponding to their maxima and minima reaches 20, whereas for n-InAs this ratio is close to the value of 2, which was found before.

Azimuthal angle dependence measurements are traditionally used for separating linear (photocurrent surge) and a nonlinear (optical rectification) contributions to the THz radiation emission. For both traces shown in Fig. 11 THz field amplitude shows a clear periodicity of cos(3θ) (θ is the azimuthal angle of the sample orientation around the axis normal to the surface) corresponding to the optical rectification effect at (111) surfaces. Such a periodicity in the (111) plane is characteristic for both bulk and electric-field-induced optical rectification, thus azimuthal angle dependencies alone cannot help by discriminating relative influences of these two effects. However, strong doping level dependence in p-InAs samples points out that, at least in this case, the prevailing physical mechanism of THz emission is the electric field-induced instantaneous polarization. Surface depletion layer width in the samples with $p=10^{17}$ cm^{-3} is approximately the same as the light absorption length at the laser wavelength (~100 nm), therefore nonlinear optical interaction due to electric-field-induced optical rectification should be most efficient in this case.

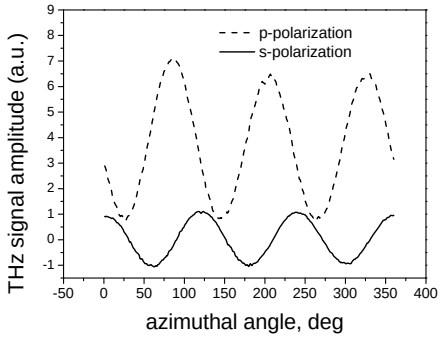

Fig. 12 The azimuthal angle dependences of the amplitude of *S*- and P- polarized THz signals measured on *n*-InAs sample with carrier density $n=2\cdot10^{16}$ cm^{-3}.

In order to clarify the dominant mechanisms, additional experiments were carried out. Emitted THz radiation dependence on azimuthal angle was measured when generating THz radiation from n-type InAs surface illuminated by a p-polarized laser radiation. Excitation intensity was 5μJ/cm^2. Studies have shown that in this case, THz radiation generated was both of p and s polarizations, which is possible only if the radiation is generated from the non-linear optical, rather than the current surge effects (Fig. 12).

On the other hand, dependences of the THz radiation efficiency from femtosecond laser illuminated InAs surfaces on the photon quantum energy lead to an opposite conclusion. The results of such measurements are presented in Fig. 13. THz field amplitude increases with the increasing photon energy, reaches maximum at $h\nu$=1.6 eV, and then decreases. Such a shape of the spectral dependence for THz emission could be expected only in the case when free electron contribution to this effect is dominating. When the quantum energy is large enough, the electrons are excited high in the conduction band, where they are efficiently scattered to the subsidiary *L* valleys with a low mobility. Intervalley separation in the conduction band of InAs determined from the experiments presented on Fig. 13 ($\Delta\varepsilon_{\Gamma L}$=1.08 eV) coincides with the previous estimations of this parameter. However, this contradicts with the previously made conclusion on the prevalence of the EFIOR effect that should not be influenced by the electron scattering rate variation. Moreover, it can be seen from Fig. 13 that the azimuthal angle anisotropy of THz amplitude at large photon energies is also decreasing as if the nonlinear optical contribution would depend on the energy of photoexcited free electrons.

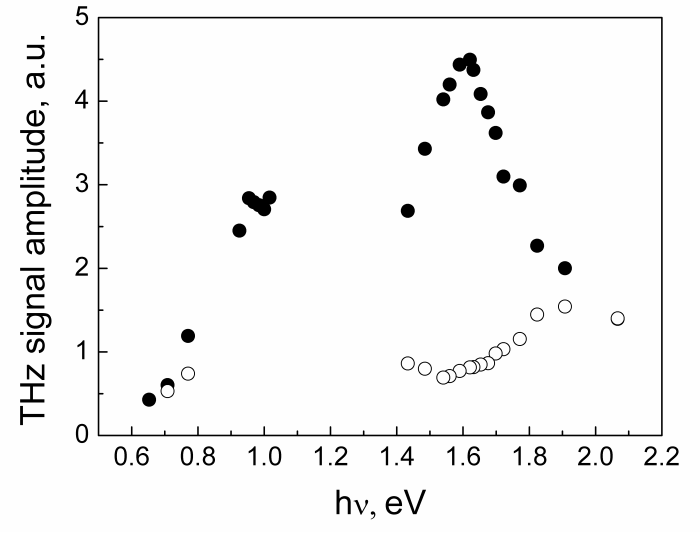

Fig. 13 THz signal radiated from InAs surface for different laser quantum energies and different azimuthal angles corresponding to minimum (open dots) and maximum (filled dots) signal amplitude. Excitation energy fluence was 10 μJ/cm^2.

Excitation of InAs by the Ti:sapphire laser pulses creates in its conduction band electrons with very large excess energies of ~1.05 eV. Therefore, at least half of the photoelectrons will move towards the bulk of the crystal at fairly high group velocities of ~ $2 \cdot 10^8$ cm/s. This motion can continue for even longer duration than the characteristic electron scattering by longitudinal optical (LO) phonons time (~100 fs) due to the peculiarities of non-parabolic conduction band structure in InAs. LO-phonon scattering will most efficiently proceed at small angles and will have little effect on electron momentum. Spatial separation of these quasi-ballistically propagating towards the bulk electrons and the holes remaining close to their excitation points will create large surface electric fields that could later interact with the optical pulse and cause the EFIOR effect and THz generation.

Because during the THz pulse generation photoexcited electrons remain hot, the dynamics of this process cannot be described using a simple drift-diffusion approach involving equilibrium electron and hole mobilities[15]. Moreover, the drift-diffusion model does not account for both the inertia of the electron dynamics and the differences in

effective masses and mobility of two distinctive groups of the electrons (equilibrium and photoexcited); peculiarities that should be important at the time scale of several hundreds of femtoseconds during which the THz pulse is generated. Therefore, numerical simulation should be used for the description of physical processes, which take place in the semiconductor immediately after its excitation by the femtosecond laser pulse. Such a simulation was made by colleague from Minsk V.L.Malevich.

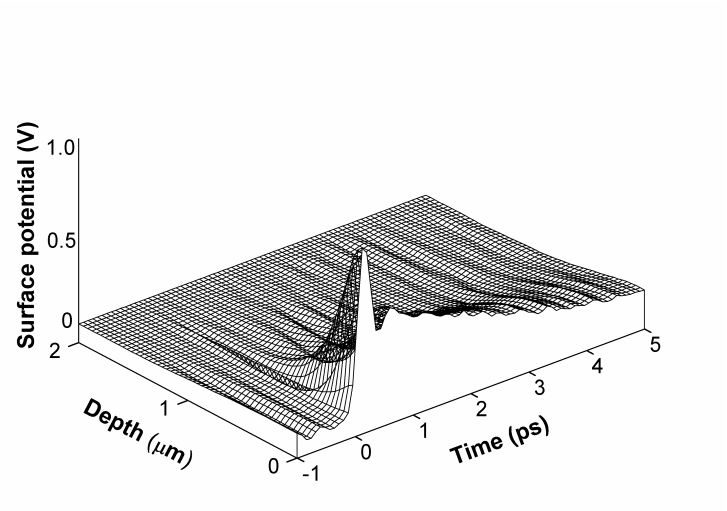

Fig. 14 Results of Monte Carlo calculation demonstrating temporal and spatial evolution of the electrical potential at the InAs surface, which was excited by 150-fs duration Ti:sapphire laser pulses.

To describe ultrafast carrier transport and subpicosecond dynamics of electric field induced at a semiconductor surface due to a spatial separation of electrons and holes excited by a short laser pulse, macro-particle method was used. The basis of this method is an ensemble Monte Carlo simulation of the particle transport in time-varying inhomogeneous electric field that is determined self-consistently from Poisson equation.

Figure 14 presents the results of the Monte Carlo calculation demonstrating temporal and spatial evolution of the electrical potential at the InAs surface, which was excited by

150-fs duration Ti:sapphire laser pulses. It can be seen from this figure that, during the excitation of the sample by the laser pulse, its surface potential changes very significantly. Electrical fields as large as $2 \cdot 10^5$ V/cm are established over distances of approximately 400 nm from the surface due to spatial separation of the electrons that are quasi-ballistically moving towards the bulk of the crystal and the holes that are more intensely scattered and remain at the vicinity of the surface.

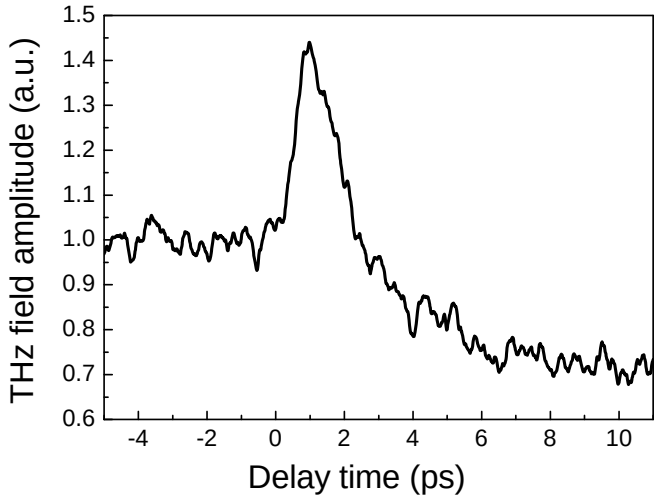

Fig. 15 . *S*-polarized component of the THz signal at its maximum as a function of the time delay between the probe and pump pulses.

Photoelectrically induced electrical fields could be larger than any static fields present at the surface of InAs, therefore, the light interaction with this field should lead to a strong EFIOR effect and to the enhancement of THz radiation from the semiconductor. As a test of this assumption, we have investigated THz emission from InAs surface induced by two optical pulses. The laser beam was split into two parts, one of which (the probe beam) was incident on the samples surface at 45^o angle and generated THz pulses monitored by the detector. The second (the pump beam) part of the laser beam was parallel to the surface normal; it was focused to a rather large spot (diameter of ~ 0.5 mm) in order to avoid

possible interference at the detector of THz pulses generated by both laser beams. Carrier densities of approximately $4 \cdot 10^{17}$ cm^{-3} and 10^{18} cm^{-3} were excited by the probe and pump beams, respectively. *S*-polarized component of the THz signal at its maximum was measured as a function of the time delay between the probe and pump pulses.

Fig. 15 shows the results of the pump-and-probe experiment. THz emission increases at times close to the overlap of both optical pulses and becomes weaker when the pump pulse arrives to the sample before the probe pulse. The effect of carriers excited by the pump pulse on THz signal generated by the probe pulse is twofold. First of all, electron ballistic movement and the charge carrier separation add to the surface electric field and leads to an increase in the generated THz signal. Secondly, when the pump pulse arrives at the surface at much earlier time moment than the probe pulse, carriers excited by the pump pulse are already cooled-down and contribute to the relaxation of the surface electrical field and to the reduction of THz generation. The shape of the experimental trace presented on Fig. 15 evidences the presence of both effects. The peak of THz emission at time close to the zero delay is due to the enhancement of the EFIOR contribution in the field induced by the pump pulse and the reduction of this emission at longer delays is, most probably, caused by the screening of the surface electrical field by the photoexcited carriers.

Even if this double-pulse excitation experiment evidences that EFIOR effect induced by the photoexcited electron movement is tangible, this does not necessary mean that it can significantly contribute to the THz emission from the surface of InAs. Enhancement of the radiated THz pulse amplitude observed at optimal conditions was only ~40%; moreover, the induced surface field in the double-pulse experiment interacts with the whole optical pulse, whereas in the case of THz pulse emission it will rectify only the tail of the optical pulse.

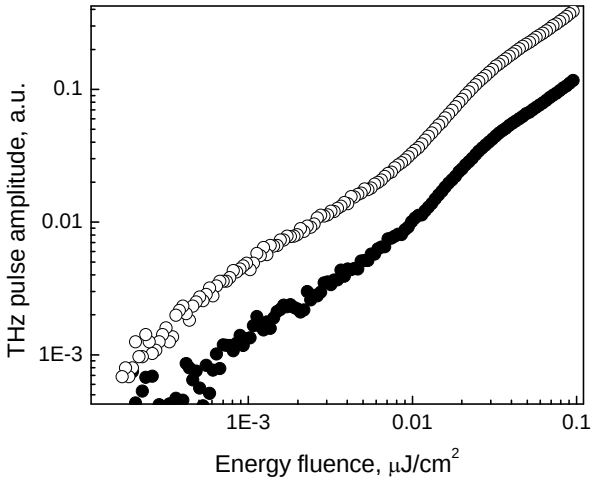

Fig. 16 THz pulse amplitudes as a function of the energy fluence measured on p-InAs (111) sample at the azimuthal angles corresponding to maximum and minimum signals.

Fig. 16 shows the amplitude of the emitted THz pulse as a function of the laser energy fluence. Both n and p-type InAs crystals (the doping level was of the order of 10^{16} cm^{-3}, the surfaces were parallel to (111) crystallographic planes) were measured at the azimuthal angles φ corresponding to the largest and the smallest THz pulse amplitudes. Dependences corresponding to the p-type InAs shown on Fig. 16 are linear (kinks at ~0.01 $\mu J/cm^2$ are caused by the nonlinearity of the neutral thin-film filter used in the experiment). THz signals measured in this experiment are P-polarized, therefore they consist of the current surge or photo-Dember effect part S_{PD} and of the EFIOR effect part, which has both φ-dependent and independent components, S_{EFIOR}. S_{EFIOR} will be proportional to the surface electric fields that will differ in differently doped crystals. The ratio of these fields in p and n-type InAs can be found directly by measuring the amplitudes of S-polarized THz pulses. In an additional experiment also performed at low photoexcitation levels, this ratio was determined as equal to $F_s^{(p)} / F_s^{(n)} = 3$.

At large fluences, the prevailing mechanism of THz generation from InAs will also be the EFIOR effect, however the main source of the surface electric field will become the photoexcited electron and hole separation. This is evidenced both by the results of Monte Carlo simulation and by the experiments performed with tunable wavelength femtosecond laser pulses (Fig. 13). THz pulse amplitudes peaking at the photon energies corresponding to the electron inter-valley separation in the conduction band indicate the importance of the free carrier dynamics, whereas a strong azimuthal angle dependence that can be observed on this figure could be attributed to the nonlinear optical effects only.

When looking for the best THz radiation emitter, $Cd_xHg_{1-x}Te$ alloys with different x were tested to determine how the generated THz radiation power depends on the semiconductor band structure. Thus, it was expected to determine what the requirements are for semiconductors, in order to have the best surface emitter. Three samples with x = 0, 0.2, 0.3 were examined during the experiments. HgTe sample was a bulk single crystal, while the remaining two were thin layers grown by epitaxy on CdTe CdHgTe substrate. These samples were compared with n-InAs sample (Fig. 17).

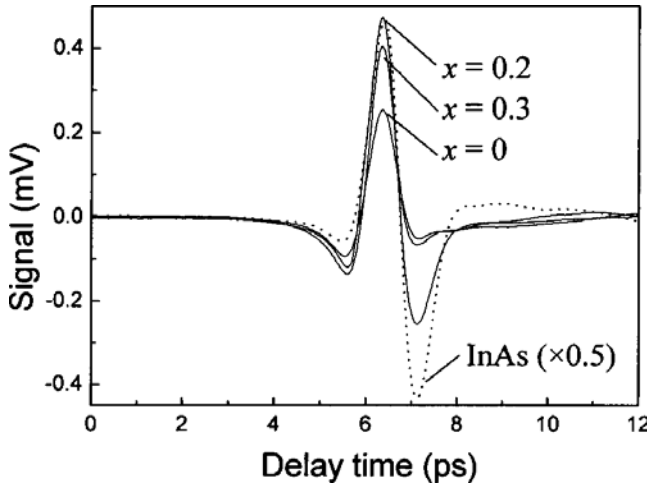

Fig. 17 THz field transients measured for the samples from different narrow-gap semiconductors.

The magnitude of the THz field radiated from both HgTe and $Cd_{0.2}Hg_{0.8}Te$ (100) surfaces does not depend on the azimuthal angle of sample orientation, which can be considered as an evidence of a prevailing role of linear processes in THz radiation from these materials.

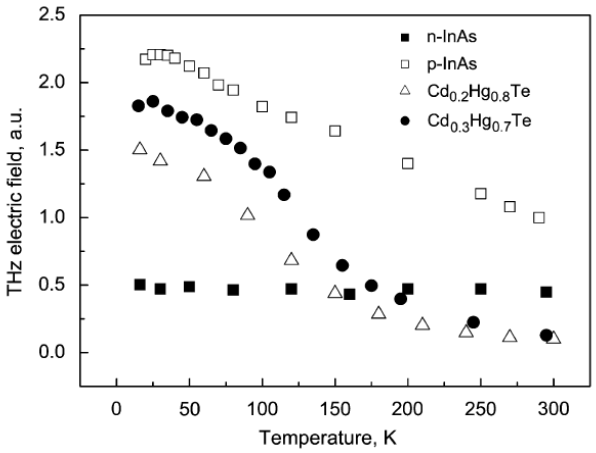

Fig. 18 THz electrical field, radiated from various semiconductor surfaces, amplitude dependence on the temperature.

Also the experiments on generation of terahertz radiation from semiconductor surfaces at low temperatures (between 300 and 15K) were performed (Fig. 18). It has been found that decreasing temperature lead to the emitted THz amplitude increase in all narrow band gap semiconductors. The reduction of the lattice temperature causes a decrease of the density and the scattering rate of the electrons, which affects the efficiency of the THz pulse generation. The largest temperature effect on the radiated THz pulse amplitude was observed in experiments with CdHgTe.

Chapter 5 describes a new method to investigate intervalley energy separation in the conduction band of a semiconductor. When looking for the most effective surface emitter, it is appropriate to measure the emitted THz semiconductor pulse amplitude dependence on the fs laser quantum energy. Such measurements in addition to purely practical significance are valuable in terms of determining semiconductor parameters. First, spectral dependences

of the THz radiation from the laser-illuminated surfaces of InAs and InSb have been investigated experimentally for the laser wavelengths ranging from 0.6 to 2 μm. Samples made from InSb (nominally undoped, $n=2\times10^{16}$ cm^{-3}, $\mu=6\times10^{4}$ $cm^2/V\ s$) and n-InAs ($n=2.2\times10^{16}$ cm^{-3}, $\mu=4.3\times10^{4}$ $cm^2/V\ s$) single crystals were investigated.

Tunable wavelength optical pulses were generated by an optical parametric amplifier and amplified Ti:sapphire laser system. The duration of the master laser pulses was 100 fs, the central wavelength was 805 nm, the single pulse energy was 1 mJ, and the pulse repetition rate was 1 kHz. The laser beam was split into two parts, the smaller of which was sent through the optical delay line to gate THz detector and the larger was used to pump parametric amplifier. Optical parametric generation was based on type II phase-matched BBO crystal. Collinearly propagating tunable wavelength signal and idler beams were generated inside that crystal. The tuning ranges of signal and idler were 1200–1610 nm and 1610–2440 nm, respectively. To obtain a radiation with the wavelengths around 800 nm, second harmonic generation using the signal or the idler beams was used. Tuning range of the second harmonic waves was 600–930 nm. The spectral range between 930 and 1200 nm was, however, inaccessible for the measurement, because the second harmonic of idler wave in this range was weak and unstable. Required wavelengths were selected by a set of dichroic mirrors; the sample's excitation power $P(\lambda)$ was kept nearly constant by means of neutral filter attenuator.

When the photon energy increases, the electrons are exited with a larger excess energy, which modifies both their velocity and the scattering rate. Especially abrupt changes in these characteristics could be expected when the photo excited electron energy reaches the position of the subsidiary valleys of the conduction band. Intense intervalley scattering will reduce the amplitude of THz signal generated both due to the photo-Dember effect and due to the optical rectification under resonant photo excitation. If one assumes that THz signal starts to decrease with increasing quantum energy hν because of the onset of the

electron transfer to large effective mass L valleys, then the energetical position of the peak could be used for the determination of the intervalley separation in the conduction band $\Delta_{\Gamma L}$. The value of this parameter is equal to the electron excess energy ε_1 and could be found from the solution of the equations describing the energy and momentum conservation in the photon absorption process:

$$\varepsilon_1 + \varepsilon_2 = h\nu - \varepsilon_g ,$$

$$\varepsilon_1 (1 + \alpha\varepsilon_1) m_e = \varepsilon_2 m_{hh} .$$

Here ε_2 is the excess energy of the photo excited heavy hole, ε_g is the energy bandgap, m_e and m_{hh} are the electron and heavy hole effective masses, and α is the coefficient for the non-parabolicity of the conduction band.

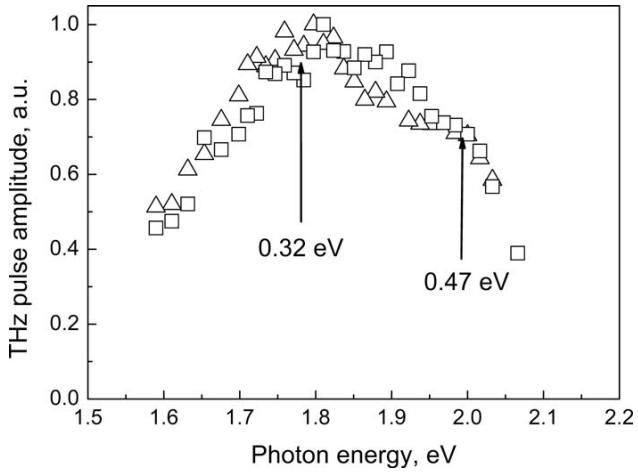

Fig. 19 Terahertz pulse amplitude dependences on the photon energy measured on (100) (squares) and (111) (triangles) crystallographic planes of GaAs. Electron excess energies corresponding to the onset of electron transitions to L and X valleys are indicated by arrows.

The intervalley separation energy calculated from experimental results for this semiconductor is $\Delta_{\Gamma L}$=0.53 eV. In the case of InAs, the intervalley separation in the

conduction band was $\Delta_{\Gamma L}$ =1.08 eV. These results can be determined from the peak of the dependence corresponding to the photon energy of 1.6 eV .

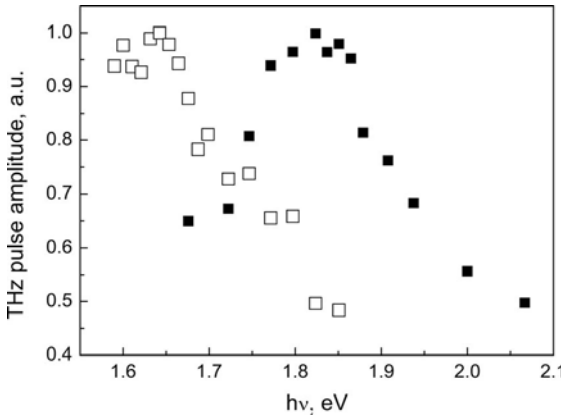

Fig. 20 Terahertz excitation spectrum measured on $Ga_{0.8}In_{0.2}As$ (full points) and $Ga_{0.47}In_{0.53}As$ (empty points) epitaxial layers.

After the first experiments showed that the method is appropriate for various semiconductors to determine the intervalley separation, InAs-InGaAs-GaAs system have been investigated at laser wavelengths ranging from 600 to 800 nm. Wide maxima evidencing the onset of the electron intervalley transfer were observed on the dependencies. It has been shown that the energy position of both the L and X conduction band valleys can be determined from the analysis of the results. Figure 19 presents the results of the measurements performed on two semi-insulating GaAs crystals cut parallel to (100) and (111) crystallographic planes. The terahertz pulse amplitudes measured at different wavelengths were normalized to a constant photon number. As it can be seen in this figure, the initial growth of the terahertz pulse amplitude in the photon energy range from 1.6 to 1.8eV is followed by its decrease at larger photon energies. Different from the results obtained on InAs and InSb, the peak of the terahertz excitation spectrum of GaAs is rather wide. Two characteristic photon energies that are indicated in Fig. 19 by the arrows can be distinguished. Slow reduction of the terahertz amplitude starts when photon energies are

equal to ~1.8 eV. This reduction becomes faster when the photon energy hν reaches the values of ~2 eV. These values can be used for the estimation of the photoexcited electron excess energies ε_1 in the Γ valley of the conduction band.

Later on, by using the procedures described above terahertz excitation spectra were measured on two $Ga_xIn_{1-x}As$ samples: lattice-matched epitaxial layer with x=0.47 grown on InP substrate and $Ga_{0.8}In_{0.2}As$ layer grown on GaAs substrate. Results of these measurements are presented in Fig. 20. The top of the spectral peaks are flat also in these cases, allowing separate estimation of the Γ-L and Γ-X intervalley energy separations in these ternary compounds. The values of those material parameters determined by taking into account the non-parabolicity of the conduction band are plotted in Fig. 21 together with the data corresponding to InAs and GaAs and compared with the widely accepted energy positions of the different conduction band minima of $Ga_xIn_{1-x}As$. As it can be seen from this figure, our results suggest that the L and X valleys in $In_xGa_{1-x}As$ are lying at higher energies as it was thought before and their energy position is changing with the composition of the alloy with only small bowing.

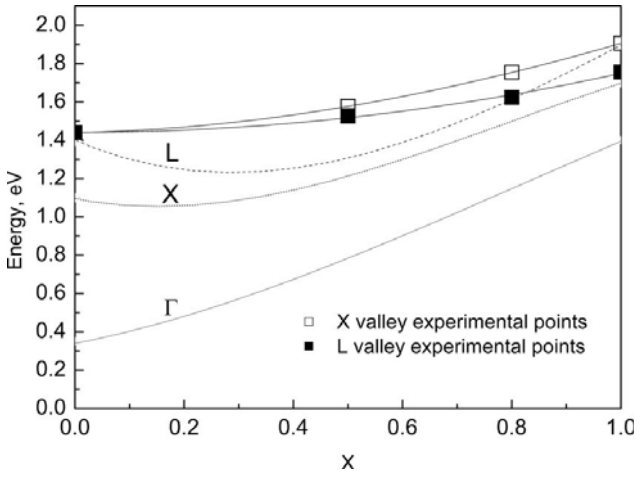

Fig. 21 Energy positions of , X, and L valleys in $Ga_xIn_{1-x}As$, vs composition parameter x. Points represent the experiment. Dashed lines are taken from http://www.ioffe.rssi.ru/SVA/NSM/Semicond/.

In the end of **Chapter 5** is concluded, that the dependences of terahertz pulse amplitude radiated from the surfaces of GaAs and two $In_xGa_{1-x}As$ alloys with different compositions as a function of the wavelength of the femtosecond laser pulses illuminating these surfaces were measured. It has been shown that the results of such measurement can be used for determining the energy position of the subsidiary L and X valleys of the conduction band of these semiconductors. The values of these parameters are of a great importance when determining the characteristics of many devices manufactured from $In_xGa_{1-x}As$ alloys: threshold fields in Gunn diodes, maximal electron drift velocity and ultimate frequency bandwidth of transistors, or barrier heights in heterostructural devices.

List of publications

1. R. Adomavičius, A. Urbanowicz, G. Molis, A. Krotkus, E. Šatkovskis, Terahertz emission from *p*-InAs due to the instantaneous poliarization, *Applied. Physics Lett*ers. **85**, 2463 (2004).
2. A. Krotkus, R. Adomavičius, G. Molis, and A. Urbanowicz, H. Eusebe, Terahertz radiation from $Cd_xHg_{1-x}Te$ photoexcited by femtosecond laser pulses, *Journal of Apllied Physics.*, **96**, 4006 (2004).
3. R.Adomavičius, S.Balakauskas, K.Bertulis, A.Geižutis, G.Molis, A.Krotkus, Low-Temperature MBE Grown GaAs for Pulsed THz Radiation Applications, *Acta Physica Polonica A*, **107**, 128 (2005).
4. R. Adomavičius, A. Urbanowicz, G. Molis, A. Krotkus, Terahertz emission from narrow gap semiconductors photoexcited by femtosecond laser pulses, *Acta Physica Polonica A*, **107**, 132 (2005).
5. A.Krotkus, G.Molis, E.Šatkovskis, Terahertz radiation from $Cd_xHg_{1-x}Te$ photoexcited by femtosecond laser pulses, *Journal of Luminescence*, **113**, 301 (2005).
6. R. Adomavičius, A. Urbanowicz, G. Molis, A. Krotkus, Terahertz radiation from narrow-gap semiconductors photoexcited by femtosecond laser pulses, *Microelectronic Engineering*, **81**, 238 (2005).

7. R. Adomavičius, G. Molis, A. Krotkus, Spectral dependencies of terahertz emission from InAs and InSb, *Applied. Physics Letters*, **87**, 1 (2005).
8. K. Bertulis, A. Krotkus, G. Aleksejenko, V. Pačebutas,a_ R. Adomavičius, and G. Molis, GaBiAs: A material for optoelectronic terahertz devices, *Applied. Physics Lett*ers, **88**, 201112 (2006).
9. G. Molis, R, Adomavičius, A. Krotkus, K. Bertulis, L. Giniūnas, J. Pocius, and R. Danielius, Terahertz time-domain spectroscopy system based on femtosecond Yb:KGW laser, *Electronics letters*, **43,** 3 (2007).
10. A. Krotkus, R.Adomavičius, G. Molis and V.L.Malevich, Terahertz Emission from InAs Surfaces Excited by Femtosecond Laser Pulses, *Nanoelectronics and Optoelectronics*, **2**, 108-114, (2007).
11. R.Adomavičius, A.Krotkus, R.Šustavičiūtė, G.Molis, J.Kois, S.Bereznev, E.Mellikov, P.Gashin, Optoelectronics surface emitters of terahertz radiation from copper chalcogenides, *Electronics Letters*, **43**, 1458-1459, (2007).
12. A. Geižutis, A. Krotkus, K. Bertulis, G. Molis, R. Adomavičius, A. Urbanowicz , S. Balakauskas, S. Valaika, Terahertz radiation emitters and detectors, *Optical Materials*, **30,** 786–788, (2008).
13. R. Adomavičius, G. Molis , A. Krotkus , V. Sirutkaitis, Excitation spectra of terahertz emission from semiconductor surfaces, *Optical Materials*, **30,** 783–785, (2008).
14. G.Molis, R.Adomavičius, A.Krotkus, Temperature-dependent terahertz radiation from the surfaces of narrow-gap semiconductors illuminated by femtosecond laser pulses, *Physica B*, **403**, 3786-3788, (2008).
15. G.Molis, A.Krotkus, and V.Vaičaitis, „Intervalley separation in the conduction band of InGaAs measured by terahertz excitation spectroscopy“, *Applied. Physics Lett*ers, **94**, 091104 (2009).

Santrauka

THz spinduliuotės generavimas iš puslaidininkių paviršiaus turi didelį potencialą puslaidininkių fizikinėms savybėms tirti. Šis darbas skiriamas puslaidininkių tyrimams generuojant THz impulsus iš jų paviršių, apšviestų femtosekundiniais lazerio impulsais. THz spinduliuotė iš puslaidininkių paviršių gali būti generuojama dėl visos eilės fizikinių mechanizmų: paviršinio lauko ekranavimo, foto-Demberio efekto, optinio lyginimo, elektriniu lauku indukuoto optinio lyginimo, plazminių svyravimų, koherentinių fononų ir plazmonų. Tiriant THz spinduliuotės generacijos mechanizmus galima išmatuoti daug svarbių puslaidininkių parametrų, tokių kaip lūžio rodiklis, judris, krūvininkų relaksacijos trukmė, aukštesniųjų laidumo slėnių padėtys. Darbo metu tirti THz spinduliuotės generacijos puslaidininkio paviršiuje mechanizmai keičiant žadinimo sąlygas: aplinkos temperatūrą, magnetinį lauką, žadinančio lazerio bangos ilgį ir intensyvumą, bei impulso trukmę. Ištyrus visą eilę įvairių puslaidininkių nustatyta, kad geriausias THz spinduliuotės emiteris žadinant 800 nm bangos ilgio spinduliuote yra p-InAs. Pirmą kartą THz žadinimo spektroskopijos metodu tiesiogiai išmatuoti tarpslėniniai atstumai $In_xGa_{1-x}As$, InAs ir InSb bandiniuose.